# Atmospheric Chemistry of 2,3-Pentanedione: Photolysis and Reaction with OH Radicals

**ARTICLE** *in* THE JOURNAL OF PHYSICAL CHEMISTRY A · AUGUST 2011

Impact Factor: 2.69 · DOI: 10.1021/jp205595c · Source: PubMed

THE JOURNAL OF PHYSICAL CHEMISTRY A

ARTICLE

pubs.acs.org/JPCA

# Atmospheric Chemistry of 2,3-Pentanedione: Photolysis and Reaction with OH Radicals

Emese Szabó,[†,‡,§,∥] Mokhtar Djehiche,[†,‡] Matthieu Riva,[†,‡] Christa Fittschen,[†,∥] Patrice Coddeville,[†,‡] Dariusz Sarzyński,[⊥] Alexandre Tomas,[*,†,‡] and Sándor Dóbé[*,§]

[†]Université de Lille Nord de France, F-59000, Lille, France

[‡]Ecole des Mines de Douai, Département Chimie et Environnement, 941 rue Charles Bourseul, 59500 Douai, France

[§]Institute of Materials and Environmental Chemistry, Chemical Research Center of the Hungarian Academy of Sciences, Pusztaszeri út 59-67, H-1025 Budapest, Hungary

[∥]PhysicoChimie des Processus de Combustion et de l'Atmosphère PC2A, UMR CNRS 8522, University of Lille 1, 59650 Villeneuve d'Ascq, France

[⊥]Department of Physical Chemistry, Wroclaw Medical University, 50-140 Wroclaw, pl. Nankiera 1, Poland

Supporting Information

**ABSTRACT:** The kinetics of the overall reaction between OH radicals and 2,3-pentanedione (1) were studied using both direct and relative kinetic methods at laboratory temperature. The low pressure fast discharge flow experiments coupled with resonance fluorescence detection of OH provided the direct rate coefficient of $(2.25 \pm 0.44) \times 10^{-12}$ cm$^3$ molecule$^{-1}$ s$^{-1}$. The relative-rate experiments were carried out both in a collapsible Teflon chamber and a Pyrex reactor in two laboratories using different reference reactions to provide the rate coefficients of $1.95 \pm 0.27$, $1.95 \pm 0.34$, and $2.06 \pm 0.34$, all given in $10^{-12}$ cm$^3$ molecule$^{-1}$ s$^{-1}$. The recommended value is the nonweighted average of the four determinations: $k_1$ (300 K) = $(2.09 \pm 0.38) \times 10^{-12}$ cm$^3$ molecule$^{-1}$ s$^{-1}$, given with $2\sigma$ accuracy. Absorption cross sections for 2,3-pentanedione were determined: the spectrum is characterized by two wide absorption bands between 220 and 450 nm. Pulsed laser photolysis at 351 nm was used and the depletion of 2,3-pentanedione (2) was measured by GC to determine the photolysis quantum yield of $\Phi_2 = 0.11 \pm 0.02(2\sigma)$ at 300 K and 1000 mbar synthetic air. An upper limit was estimated for the effective quantum yield of 2,3-pentanedione applying fluorescent lamps with peak wavelength of 312 nm. Relationships between molecular structure and OH reactivity, as well as the atmospheric fate of 2,3-pentanedione, have been discussed.

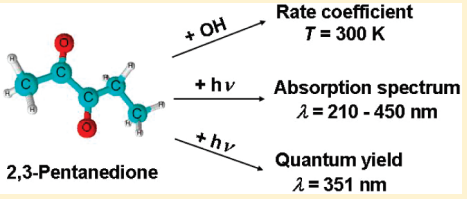


## 1. INTRODUCTION

2,3-Pentanedione ($CH_3C(O)C(O)CH_2CH_3$, 2,3PD) is a constituent of natural fragrances and synthetic flavoring agents, a selective polar solvent, and a starting material for the manufacture of dyes and pharmaceuticals.[1] It is volatile enough to escape into the atmosphere where it is expected to react primarily with OH radicals and to undergo photolysis. 2,3PD belongs to the family of α-dicarbonyls, several of which are of great importance for the chemistry of the troposphere, including glyoxal, C(O)(H)C(O)(H), methyl-glyoxal, $CH_3C(O)C(O)H$, and biacetyl, $CH_3C(O)C(O)CH_3$. While these latter oxygenates have been the subjects of numerous reaction kinetic and photochemical studies, see, for example, refs 2−4 and refs 5−7, respectively, no such studies have been reported for 2,3PD in the homogeneous gas phase.

We have performed reaction kinetic and photochemical investigations of 2,3-pentanedione. The objectives of the present study were to improve our understanding of the effect of vicinal carbonyl groups on the reactivity with OH radicals and to asses the atmospheric fate of the potentially important volatile organic compound (OVOC), 2,3PD. In this paper we present rate coefficients for the overall reaction of 2,3PD with OH radicals, $k_1$, absorption cross sections as a function of wavelength, $\sigma_{2,3PD}(\lambda)$, photolysis rate coefficients, $J_2$, and quantum yield, $\Phi_2$, at selected wavelengths, all of them determined at laboratory temperature ($T \approx 300$ K).

$$OH + CH_3C(O)C(O)CH_2CH_3 \rightarrow \text{products} \quad k_1 \qquad (1)$$

$$CH_3C(O)C(O)CH_2CH_3 + h\nu \rightarrow \text{products} \quad \Phi_2 \text{ and } J_2 \qquad (2)$$

Experiments were carried out both in the Chemical Research Center, Budapest (CRC, Budapest), and the École des Mines de Douai (EMD, Douai) by employing the complementary experimental techniques that are available at the two research sites.

**Received:** April 30, 2011
**Revised:** July 21, 2011
**Published:** July 25, 2011

Thus, kinetic experiments were carried out using the direct discharge flow method and using also relative-rate techniques to obtain rate coefficient for reaction (1). Photolysis experiments were performed employing both a pulsed laser at 351 nm and a continuous broadband irradiation source at 312 nm. The kinetic and photochemical data we present are believed to be the first determinations in the literature and, apart from the work of Jackson and Yarwood,[8] no absorption spectrum for 2,3PD has been reported.

## 2. EXPERIMENTAL SECTION

**Discharge Flow Technique.** Absolute rate coefficient for the reaction OH + $CH_3C(O)C(O)CH_2CH_3$ (1) was determined in Budapest by using the low pressure fast discharge flow technique (DF) coupled with resonance fluorescence detection (RF).[9,10]

The flow-tube reactor was constructed of Pyrex and had an inner diameter of 4.0 cm and an overall length of 60 cm. The internal surface of the reactor was coated with a thin film of halocarbon wax to reduce heterogeneous loss of OH radicals. The reactor was equipped coaxially with a movable injector; helium was the carrier gas. OH radicals were produced inside the injector by reacting H atoms with a slight excess of $NO_2$: H + $NO_2 \rightarrow$ OH + NO; H atoms were generated by microwave discharge of trace $H_2$ in helium flow. 2,3-Pentanedione was used, premixed in helium, from blackened bulb reservoirs and the concentration of the mixture was checked by GC or UV−vis absorption before use.

The OH(A−X) excitation radiation was produced by a microwave powered resonance lamp operated with flowing $Ar/H_2O$ at low pressure. The RF radiation emerging from the detection cell was passed through an interference filter centered at 307 nm and detected by a photomultiplier. The minimum detectable OH concentration was approximately $2 \times 10^9$ molecules $cm^{-3}$.

**Relative-Rate Experiments Using a Pyrex Reactor.** Kinetic experiments were performed in a 10 L Pyrex bulb, PR, to determine relative rate coefficient for reaction (1) in Budapest (RR-PR experiments). OH radicals were produced by the photooxidation of $CH_3ONO$ in synthetic air. The photolytic light source was a modified movie projector operated with a 3 kW Xe arc. The irradiating light was passed through a heat reflecting mirror and three liquid filters of 12 cm optical path each in the following order: water, an aqueous solution of chrome alum, and an aqueous solution of methylene blue.[11] The transmitted light had a bell-shaped intensity profile with a maximum at $\lambda_{max}$ = 362 nm and a full width at half-maximum of $w$ = 28 nm.

The reaction mixtures contained $(5.6 - 6.0) \times 10^{15}$ molecules $cm^{-3}$ 2,3PD, $(7.9 - 8.5) \times 10^{15}$ molecules $cm^{-3}$ MEK (methyl ethyl ketone, reference reactant), $1.0 \times 10^{15}$ molecules $cm^{-3}$ $c$-$C_4F_8$ (GC standard), $\sim 4 \times 10^{16}$ molecules $cm^{-3}$ methyl nitrite, and synthetic air made up to 1050 mbar overall pressure. The reaction temperature was measured inside the reactor using a retractable thermocouple. It was found constant and slightly above the ambient temperature ($T$ = 302 ± 4 K). Samples for analysis were withdrawn by a gastight syringe through a septum connected to a thin glass tube which reached in the middle of the bulb. Concentrations were determined by isothermal GC and flame ionization detection (FID). The GC parameters are given in Table SI-2 in the Supporting Information.

**Relative-Rate and Photochemical Experiments Using a Collapsible Teflon Reactor.** A collapsible Teflon reactor, TR, was used at Douai[12] to determine relative rate coefficients for reaction 1, as well as to obtain photolysis rate coefficients for 2,3PD, $J_2$. The reactor had a volume of ∼250 L. Two types of fluorescent tubes were used for irradiation: Vilbert-Lourmat T-20 M (20 W) with peak intensity at $\lambda_{max}$ = 312 nm and $w$ = 11 nm, as well Philips TL-K (40 W) with $\lambda_{max}$ = 365 nm and $w$ = 34 nm.

Most of the reactants were volatile liquids (2,3PD, MEK, etc.), measured amounts of which were injected in a small evacuated glass vessel first, and were then flushed into the Teflon-bag reactor one by one with a stream of purified air. In the final step, the reactor was filled to its full volume with air (or $N_2$ in the case of $NO_2$ photolysis). Concentration depletion of the organics was measured at regular intervals using online GC-FID analysis (Table SI-2 in the Supporting Information).

The following were the initial concentrations: OH-reaction (RR-TR experiments), $[2,3PD]_0 = (1.2 - 3.0) \times 10^{14}$ molecules $cm^{-3}$, $[ethanol]_0 = 4.3 \times 10^{14}$ molecules $cm^{-3}$ (reference reactant), $[MEK]_0 = (2.8 - 4.2) \times 10^{14}$ molecules $cm^{-3}$ (reference reactant), and $[CH_3ONO]_0 \approx 1 \times 10^{16}$ molecules $cm^{-3}$ (OH radical source); continuous photolysis (CP-TR experiments): $[2,3PD]_0 = (2.5 - 6.5) \times 10^{14}$ molecules $cm^{-3}$.

In the $NO_2$ actinometry measurements, the photolysis rate coefficient, $J_{NO_2}$, was determined at 312 nm by monitoring the consumption of $NO_2$ during the irradiation of dilute $NO_2/N_2$ mixtures; the initial concentration was $[NO_2]_0 \approx 8 \times 10^{13}$ molecules $cm^{-3}$. A calibrated commercial $NO_x$ analyzer was used for the concentration measurements, which was operated continuously by sampling a small flow of the irradiated gas mixture from the Teflon bag.

**Measurements of Absorption Cross Sections.** The UV−vis absorption spectrum of 2,3PD was determined in Budapest employing a home-built gas spectrophotometer.[14] Briefly, the light beam of a $D_2$ lamp was passed through a 50.2 cm absorption cell thermostatted to $T$ = 298 ± 1 K, dispersed by a 0.25 m monochromator, and detected by a photomultiplier interfaced to a lock-in amplifier and PC. The spectral resolution was ∼0.4 nm. The light intensity was strongly reduced by using neutral filters to minimize potential photolysis of the analyzed samples.

**Laser Photolysis Technique.** Pulsed laser photolysis (PLP) at 351 nm was used to determine photolysis quantum yield for 2,3PD, $\Phi_2$(351 nm) in Budapest. The concentration depletion was determined after a measured number of laser shots using GC analysis.[13,14]

An exciplex laser provided the pulsed laser light; the laser was operated at 5 Hz. Photolysis was performed in a 11.6 (optical path) × 3.6 cm (internal diameter) cylindrical quartz cell (PLP-QR experiments). A septum joint was attached to the cell for GC sampling (Table SI-2). The laser energy was measured using a calibrated laser energy meter; the energy was typically ∼20 mJ $pulse^{-1}$. The photolysis was carried out in synthetic air with mixtures containing $6.3 \times 10^{15}$ molecules $cm^{-3}$ 2,3-pentanedione and $1.5 \times 10^{15}$ molecules $cm^{-3}$ $c$-$C_4F_8$.

**Chemicals.** 2,3PD was purchased from Merck and Sigma-Aldrich with the nominal purities of ≥98 and 97%, respectively. The samples were purified by multiple trap-to-trap distillations in vacuum (6×), retaining ∼2/3 middle fraction at each step. Purity of the distilled 2,3PD was 98.5% in the liquid phase and ≥99.5% in the gas phase. MEK (Sigma-Aldrich, >99.7%), $c$-$C_4F_8$ (PCR Inc., 99%), methanol (Merck, 99.9%) and ethanol (Merck, 99.9%) were degassed by several freeze−pump−thaw cycles prior to use. Most of the gases were used as obtained: $H_2$ (99.95%, Messer-Griesheim), He (99.996%, Messer-Griesheim), synthetic air (Messer Hungaria, ≥ 99.5%), zero-grade air (Claind

Type AZ 2000 generator). $NO_2$ (Messer-Griesheim, 98%) was purified by repeated trap-to-trap distillations in vacuum from slurries kept at low temperatures. Methyl nitrite, $CH_3ONO$, was prepared from methanol with nitrous acid[15] and was purified by trap-to-trap distillations.

**Errors.** Unless otherwise stated, the quoted uncertainties are two standard deviations throughout the paper and represent precision only. The errors are typically those that have returned from regression analyses and have always been propagated for the derived quantities.

## 3.1. KINETIC RESULTS AND DISCUSSION

**3.1.1. DF-RF Determination of $k_1$.** The experiments were conducted at $T = 300 \pm 3$ K reaction temperature and $P = 2.49 \pm 0.06$ mbar He pressure. The standard pseudo-first-order kinetic method was employed to determine absolute rate coefficient for OH + $CH_3C(O)C(O)CH_2CH_3$ (1) with a large excess of [2,3PD] over the hydroxyl radical concentration of $[OH]_0 \approx 3 \times 10^{11}$ molecules $cm^{-3}$. The experiments were performed by recording the OH resonance fluorescence signal strengths versus the varied reaction distance, $z$, with, $S^{OH}_{on}$, and without, $S^{OH}_{off}$, of the reactant 2,3-pentanedione flow. Under the plug-flow condition of the low-pressure DF technique, the reaction time equals $z \times v_{lin}^{-1}$, where $v_{lin}$ is the average linear flow velocity in the flow tube. The bimolecular reaction between OH and 2,3PD was kinetically isolated from the interfering reactions in the homogeneous gas phase, but the consumption of OH was significant on the surface of the reactor, which was found to obey first-order kinetics with an effective "wall rate coefficient" of $k_w$.

Therefore, assuming pseudo-first-order kinetics and with the provision that the wall activity for OH was not very different in the presence and absence of 2,3PD, the experimental observables were evaluated by the eqs I–III:

$$-\ln \frac{S^{OH}_{on}}{S^{OH}_{off}} = k_1' \frac{z}{v_{lin}} \quad \text{(I)}$$

$$k_1' = k_1[2,3PD] + \text{const} \quad \text{(II)}$$

$$-\ln S^{OH}_{off} = k_w \frac{z}{v_{lin}} \quad \text{(III)}$$

The measured hydroxyl decays, when plotted according to eq I, displayed straight lines, indicating the validity of first-order kinetics. The slopes provided the pseudo-first-order rate coefficient, $k_1'$, by linear least-squares analysis (LSQ). Sample decay plots are shown in the inset of Figure 1. The main panel of this figure shows a plot of $k_1'$ versus [2,3PD] (eq II); the bimolecular rate coefficient, $k_1$, was obtained as LSQ slope. The plotted ln $S^{OH}_{off}$ versus $z$ data gave also straight lines, the slopes of which supplied $k_w$ (eq III).

Large heterogeneous effects were observed in the first experiments portrayed by very high OH consumption on the surface of the reactor and a smaller than expected signal magnitudes in the experiments that were carried out in close succession to each other. Such effects are indicative of the adsorption of 2,3PD on the walls of the reactor and an enhanced heterogeneous reaction with the OH radicals. Similar behavior was reported by Stevens and co-workers for discharge flow reactions of OH with different polar reactants including carbonyls (see, e.g., ref 16 and references therein). These authors have reported the heterogeneous

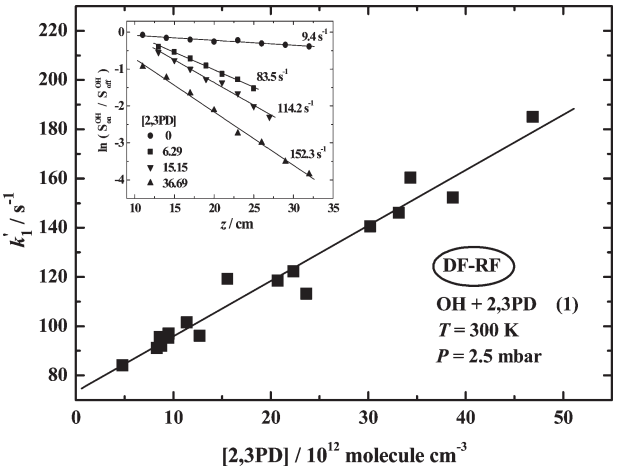


**Figure 1.** Plots used to determine $k_1$. The figure in the inset shows representative OH-decays vs the reaction distance, where $S^{OH}_{on}$ and $S^{OH}_{off}$ are the OH signal strengths with and without 2,3PD flow, respectively, and the 2,3PD concentrations are given in $10^{12}$ molecules $cm^{-3}$.

effects to be minimized by the addition of $O_2$. However, this option was not feasible in our current experiments because a substantial reformation of OH was observed when oxygen flow was added to the reaction system that might have caused an underestimation of the rate coefficients in the measurements. Long evacuation time and conditioning of the walls of the flow tube with OH radicals were used prior to each experiment. In this way, reasonable reproducibility was achieved, but the bimolecular rate coefficient plot showed a significant intercept (Figure 1), and the $k_w = 7–47$ $s^{-1}$ values were somewhat larger than the usual wall consumption of OH ($\sim 3–20$ $s^{-1}$) that we observed previously in DF experiments with inert wall coatings.

The experimental conditions and kinetic results are summarized in Table 1. We have not corrected the measured rate coefficient for viscous flow and axial diffusion in the present work. Instead, an 8% contribution was included in the error margins to account for such effects and other potential systematic errors by experience with previous reaction systems. Thus, the following rate coefficient is proposed by the DF-RF study for the reaction of OH radicals with 2,3-pentanedione: $k_1(300\ K) = (2.25 \pm 0.44) \times 10^{-12}$ $cm^3$ molecule$^{-1}$ $s^{-1}$ given with an overall uncertainty at the $2\sigma$ level.

**3.1.2. Relative-Rate Kinetic Studies.** Relative rate coefficients for the reaction of OH with 2,3-pentanedione were determined by comparing the rate of loss of the substrate to that of a reference compound the rate coefficient for which is accurately known. 2,3PD was found to photolyze slowly at the wavelengths used to produce OH, however, no loss of the reference compounds at the time scale of the kinetic experiments was observed by test irradiations conducted in the absence of 2,3PD and the OH-source $CH_3ONO$.

$$\text{OH} + \text{2,3-pentanedione} \rightarrow \text{products}, \quad k_1 \quad (1)$$

$$\text{OH} + \text{reference} \rightarrow \text{products}, \quad k_{ref} \quad (\text{ref})$$

$$\text{2,3-pentanedione} + h\nu \rightarrow \text{products}, \quad J_2 \quad (2)$$

$\lambda_{max} = 362$ and 365 nm.

**Table 1. Summary of Experimental Conditions and Results for the Reaction OH + 2,3PD (1) Using the DF-RF Method ($T$ = 300 ± 3 K, $P$ = 2.49 ± 0.06 mbar He Buffer Gas)[a]**

| $\nu_{lin}$ (cm s$^{-1}$) | $[OH]_0$ ($10^{11}$ molecules cm$^{-3}$) | [2,3PD] ($10^{12}$ molecules cm$^{-3}$) | $k_w$ (s$^{-1}$) | $k_1'$ (s$^{-1}$) | No. of expts | $k_1$ ($10^{-12}$ cm$^3$ molecule$^{-1}$ s$^{-1}$)[a] |
|---|---|---|---|---|---|---|
| 874−1055 | 2−10 | 4.79−46.9 | 7−47 | 84−185 | 17 | 2.25 ± 0.24 |

[a] The errors represent 2$\sigma$ statistical uncertainties.

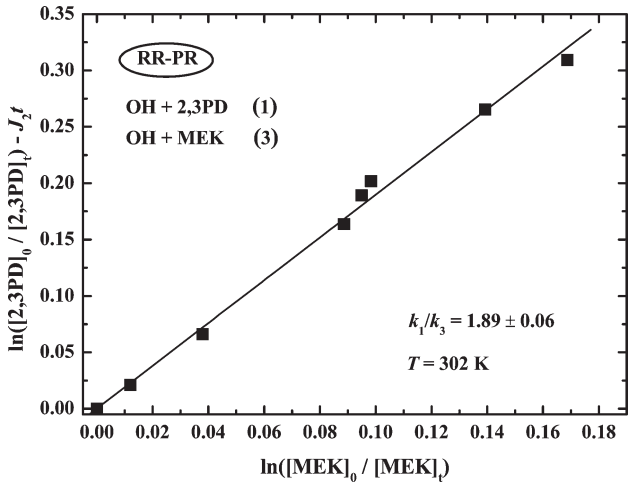


**Figure 2.** Plot used to determine rate coefficient ratio for the reaction of OH radicals with 2,3PD obtained from measurements using the Pyrex reactor and MEK as the reference reactant.

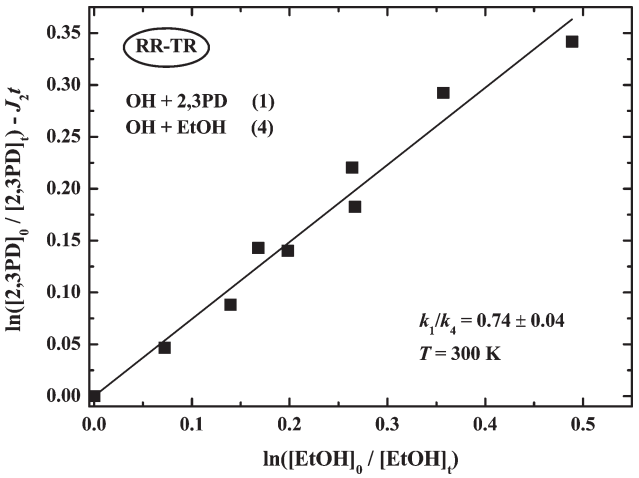


**Figure 3.** Plot used to determine rate coefficient ratio for the reaction of OH radicals with 2,3PD obtained from measurements using the Teflon bag reactor and EtOH as the reference reactant.

Provided that 2,3PD and the reference compounds are lost only by reactions with OH, neither 2,3PD, nor the reference compounds are reformed in the systems and that the photolysis of 2,3PD is slow compared to the studied chemical reactions, the following expression is obtained

$$\ln\{[2,3\mathrm{PD}]_0/[2,3\mathrm{PD}]_t\} - J_2 \times t = (k_1/k_{\mathrm{ref}}) \times \ln\{[\mathrm{ref}]_0/[\mathrm{ref}]_t\} \quad \text{(IV)}$$

where $[2,3PD]_0$, $[2,3PD]_t$, $[ref]_0$, and $[ref]_t$ are the concentrations of the 2,3PD and reference at time zero and $t$, $J_2$ is the photolysis rate coefficient determined from separate experiments, $t$ is the reaction time, $k_1$ and $k_{ref}$ are the rate coefficients for the 2,3PD reaction and the reference reaction, respectively. Thus, plots of the left-hand side of eq IV versus ln $\{[ref]_0/[ref]_t\}$ should be linear with zero intercept and slope equal to $k_1/k_{ref}$.

OH radicals were produced by the photolysis of methyl nitrite in air

$$\mathrm{CH_3ONO} + h\nu \rightarrow \mathrm{CH_3O} + \mathrm{NO} \quad (\lambda_{\max} = 362 \text{ and } 365 \text{ nm})$$

$$\mathrm{CH_3O} + \mathrm{O_2} \rightarrow \mathrm{HO_2} + \mathrm{HCHO}$$

$$\mathrm{HO_2} + \mathrm{NO} \rightarrow \mathrm{OH} + \mathrm{NO_2}$$

*RR-PR Determination of $k_1$.* Relative-rate kinetic experiments were carried out in synthetic air, at $T$ = 302 ± 4 K reaction temperature and 1050 mbar overall pressure, using the Pyrex reactor. The reaction with methyl ethyl ketone, OH + MEK (3), served as reference. The measured concentration ratios plotted according to eq IV are presented in Figure 2. The photolysis rate coefficient needed for the data evaluation was determined by measuring the photodepletion of 2,3PD in the absence of $CH_3ONO$ and MEK but, otherwise, under the same experimental conditions. Single exponential time dependence was observed providing $J_2(362 \text{ nm}) = (1.99 \pm 0.32) \times 10^{-5}$ s$^{-1}$ as the decay constant. This photolysis rate has resulted in a maximum correction of ~9% of the OH-reaction in eq IV. Linear least-squares analysis of the data plotted in Figure 2 have supplied $k_1/k_3 = 1.89 \pm 0.06$. The rate coefficient ratio has been put to an absolute scale by taking $k_3 = (1.09 \pm 0.18) \times 10^{-12}$ cm$^3$ molecule$^{-1}$ s$^{-1}$ from ref 17 to give $k_1 = (2.06 \pm 0.34) \times 10^{-12}$ cm$^3$ molecule$^{-1}$ s$^{-1}$. (The rate coefficient value we use for the reference reaction agrees within 10% with those recommended by the IUPAC and JPL data evaluations.[18,19])

*RR-TR Determination of $k_1$.* Two reference reactions, OH + MEK (3) and OH + $C_2H_5OH$ (EtOH; 4), were used in the relative-rate experiments that were performed in the Teflon-bag reactor. The reaction conditions were: $T$ = 300 ± 2 K and $P$ = 1000 mbar overall pressure synthetic air. Similar to the Pyrex-reactor experiments, photolysis loss of 2,3PD had to be taken into account in deriving the rate coefficient ratios. The photolysis rate coefficient has been determined to be $J_2(365 \text{ nm}) = (2.01 \pm 0.08) \times 10^{-5}$ s$^{-1}$; the correction for photolysis was less than 15%. A plot according to eq IV is presented in Figure 3 displaying results with the application of the EtOH reference reaction. An LSQ slope of the straight line of Figure 3 provides $k_1/k_4 = 0.74 \pm 0.04$, which is resolved to the absolute rate coefficient of $k_1 = (1.95 \pm 0.27) \times 10^{-12}$ cm$^3$ molecule$^{-1}$ s$^{-1}$ by taking $k_4 = (3.2 \pm 0.4) \times 10^{-12}$ cm$^3$ molecule$^{-1}$ s$^{-1}$ from ref 18.

Well-obeyed straight line with zero intercept similar to those shown in Figures 2 and 3 was obtained also with the application

of the methyl ethyl ketone reference reaction[17] in the Teflon-reactor experiments supplying $k_1/k_3 = 1.79 \pm 0.11$ and $k_1 = (1.95 \pm 0.34) \times 10^{-12}$ cm$^3$ molecule$^{-1}$ s$^{-1}$. The relative-rate plot obtained with the OH + MEK (3) reference reaction is presented as Figure SI-2 in the Supporting Information.

**3.1.3. Reactivity of 2,3-Pentanedione with OH.** The absolute and relative-rate kinetic studies have provided rate coefficients for reaction (1) in good agreement with each other: DF-RF, 2.25 ± 0.44; RR-PR, 2.06 ± 0.34; RR-TR, 1.95 ± 0.27 and 1.95 ± 0.34, all given in $10^{-12}$ cm$^3$ molecule$^{-1}$ s$^{-1}$. Note also that $k_1$ has been found invariant to the reaction pressure in a wide range between ~2 and ~1000 mbar. The good agreement lends credence to the reliability of the results in particular that they were obtained from independent measurements in two laboratories using different experimental techniques. The recommended rate coefficient for the reaction of OH radicals with 2,3PD is the nonweighted average of the $k_1$ determinations:

$$k_1(300\ \mathrm{K}) = (2.09 \pm 0.38) \times 10^{-12}\ \mathrm{cm^3\ molecule^{-1}\ s^{-1}}$$

given with an overall accuracy proposed to be valid at the 95% confidence level.

To our knowledge, no prior rate coefficient has been reported for reaction (1). The only other α-diketone that has been a subject of OH-kinetic study is 2,3-butanedione ($CH_3C(O)C(O)CH_3$, or biacetyl). A rate coefficient of $(2.3 \pm 0.2) \times 10^{-13}$ cm$^3$ molecule$^{-1}$ s$^{-1}$ ($T$ = 298 K) has been determined by Dagaut et al.[4] for the OH + biacetyl reaction in good agreement with a previous measurement by Darnall et al.[20] The rate coefficient we propose from our current work for the OH + $CH_3C(O)C(O)CH_2CH_3$ (1) reaction is ~10 times higher, which can be rationalized, however, by the increased reactivity of the $CH_2$ group not present in the biacetyl molecule (see below).

A structural isomer of 2,3PD is 2,4-pentanedione (2,4PD), which is a β-diketone. Holloway and co-workers have carried out a detailed kinetic study of the reaction of OH with 2,4PD using both direct and relative kinetic methods.[21] The rate coefficient they have reported is $(8.78 \pm 0.58) \times 10^{-11}$ cm$^3$ molecule$^{-1}$ s$^{-1}$ ($T$ = 298 K), which is more than 40 times higher than the $k_1$ value we have determined for the OH + $CH_3C(O)C(O)CH_2CH_3$ (1) reaction. Holloway et al.[21] have explained the high rate coefficient by that 2,4-pentanedione exists in the gas phase predominantly as the enol tautomer, $CH_3C(O)CH{=}C(OH)CH_3$, which undergoes fast addition reaction with the OH radical, while the keto-form ketones react via the slower hydrogen abstraction reaction. In contrast to 2,4PD, the vicinal diketone 2,3PD exists predominantly in the keto form with the enol form being present to a few percentages, at the most, in the gas phase at room temperature.[22,23]

The reactivity properties of 2,3PD can be understood by the considerable knowledge that has been gathered throughout the years for the kinetics and mechanism of the reactions of OH radicals with the aliphatic monoketones, see, for example, refs 24 and 25 and also the review paper by Mellouki et al.[26] The C=O group slightly reduces the bond dissociation energy (BDE) of a neighboring C−H bond,[19] but it is strongly electron withdrawing, which overrides the BDE-reducing effect, and so hydrogen abstraction by the electrophilic OH radical becomes less facile at the α-position.[26,27] On the other hand, a characteristic feature of the OH reactions of $C_n \geq 3$ ketones is the increased reactivity of the C−H bonds at the β-position.[25,26] This latter effect is thought to be the decisive factor in determining the pronounced reactivity of 2,3PD toward OH, compared, for example, with propane, $CH_3CH_2CH_3$, which has the same number and types of H atoms, but its rate coefficient is about half of that of the 2,3PD reaction ($k$(OH + propane) = $1.1 \times 10^{-12}$ cm$^3$ molecule$^{-1}$ s$^{-1}$, $T$ = 298 K[19]).

An important development for understanding the reactivity of OH radicals with polar organic molecules, including carbonyls, has been the recognition of the important role that weakly bound 'prereaction' (or 'prereactive') complexes play in the molecular mechanisms of the reactions, as it has been reviewed[28−30] and discussed in detail, for example, in refs 31 and 32. Specifically, the role of hydrogen bonded complexes in enhancing the reactivity of the β-C−H bond in the reactions of OH with aliphatic ketones has been assessed by Alvarez-Idaboy and co-workers by quantum chemical and theoretical reaction kinetics computations.[32] They have shown that the β-prereaction complexes, C=O···HO··$\cdot$H$_\beta$C$_s$, significantly lower the reaction barrier via hydrogen-bond-like interactions in the transition state thus leading to increased rate coefficients.

One of the most frequently used methods to estimate OH reaction rate coefficients for gas-phase organic compounds has been Atkinson's structure−reactivity (SAR) approach,[27] which was found to work very well for the OH + aliphatic ketones reactions.[24] According to the SAR procedure, the total rate coefficient for the reaction OH + $CH_3C(O)C(O)CH_2CH_3$ (1) can be estimated as the sum of the following group rate coefficients ($T$ = 298 K):

$$k_1 = k_{\mathrm{prim}}F(>\mathrm{CO}) + k_{\mathrm{sec}}F(>\mathrm{CO})F(-\mathrm{CH_3}) + k_{\mathrm{prim}}F(-\mathrm{CH_2C(O)}-) \quad \text{(V)}$$

where $k_{\mathrm{prim}}$ and $k_{\mathrm{sec}}$ are the rate coefficients per $CH_3-$ and $-CH_2-$ groups and $F$s are the substituent factors. Taking the tabulated generic rate coefficients $k_{\mathrm{prim}}$, $k_{\mathrm{sec}}$ and the substituent factors from ref 27 one obtains $k_1 = 1.33 \times 10^{-12}$ cm$^3$ molecule$^{-1}$ s$^{-1}$, which is an ~50% underestimate of the experimental value. We believe the reason is simply that the substituent factors currently available do not reflect the activating effect of a −C(O)C(O)− moiety on the β-C−H bond. Conversely, a $F(-C(O)C(O)-)$ factor can be derived by using our measured rate coefficient and the group reactivity parameters given in ref 27.

$$k_1(\mathrm{meas}) = k_{\mathrm{prim}}F(-\mathrm{C(O)C(O)}-) + k_{\mathrm{sec}}F(-\mathrm{C(O)C(O)}-)F(-\mathrm{CH_3}) + k_{\mathrm{prim}}F(-\mathrm{CH_2C(O)}-) \quad \text{(VI)}$$

This estimation provides $F(-C(O)C(O)-) = 1.55$, which indicates a definite, but smaller, activating effect than that of the $-CH_2C(O)-$ group, $F(-CH_2C(O)-) = 3.9$.[27]

## 3.2. PHOTOCHEMICAL RESULTS AND DISCUSSION

**3.2.1. UV−Vis Absorption Spectrum of 2,3-Pentanedione.** The absorption spectrum for 2,3PD was determined over the wavelength range of $\lambda$ = 210−450 nm, at room temperature ($T$ = 298 ± 1 K). The wavelength-dependent cross sections, $\sigma_{2,3\mathrm{PD}}(\lambda)$, were obtained from absorption measurements applying the Beer−Lambert law:

$$\ln\{(I_0)/(I)\} = \sigma_{2,3\mathrm{PD}}(\lambda)\ell[2,3\mathrm{PD}] \quad \text{(VII)}$$

where $\ell$ (= 50.2 cm) is the optical path length, and $I_0$ and $I$ are the

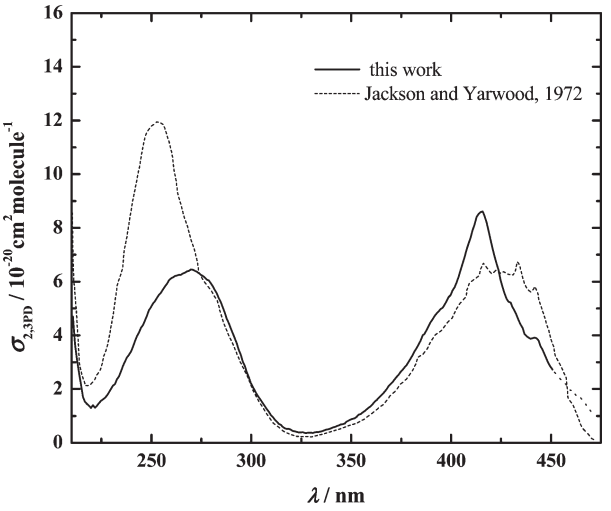


**Figure 4.** Absorption spectrum of 2,3-pentanedione in the gas phase at laboratory temperature: (—), this work; (····), Jackson and Yarwood.[8].

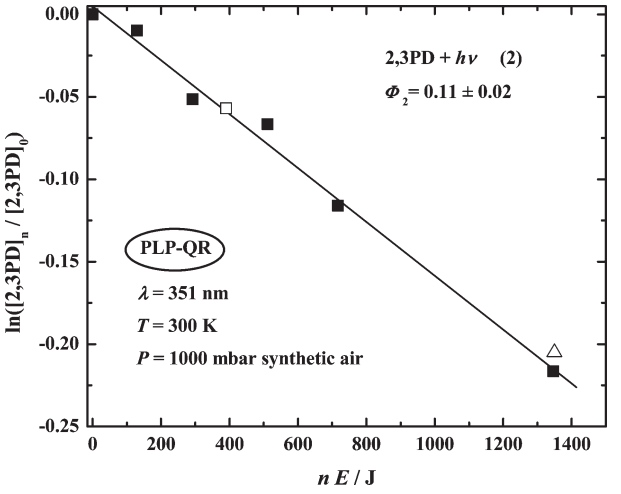


**Figure 5.** Depletion of 2,3PD concentration in pulsed laser photolysis experiments: $n$ is the number of laser shots and $E$ is the energy per pulse. The slope is proportional to the $\Phi_2$(351 nm) photolysis quantum yield. The open symbols designate experiments performed with reaction mixtures containing 1-pentene as an OH scavenger.

transmitted light intensities in the absence and presence of 2,3PD, respectively. The spectrum is shown in Figure 4 and the corresponding absorption cross sections, $\sigma_{2,3PD}(\lambda)$, are tabulated in 1 nm intervals in the Supporting Information (Table SI-1) where representative Beer−Lambert (BL) plots are also presented (Figure SI-1).

As a first step, survey spectra were taken using the 2,3PD, as obtained from the supplier (nominally ≥98% purity sample). One of the characteristic features of the spectrum determined was a strong absorption band at ∼250 nm, which had a shoulder at ∼270 nm. The 250 nm peak disappeared, however, when the spectrum was recorded with the purified sample and a lower-intensity unstructured band emerged with a maximum at 270 nm. The short-wavelength feature of the spectrum appeared again when the 2,3PD/He mixture applied for the analysis was prepared and stored in a bulb, which was used previously for storing other organics in gas mixtures, indicating the potential chemical transformation of 2,3PD on contaminated surfaces. Therefore, new, carefully cleaned glass parts were installed, and the absorption spectra were taken with the purified 2,3PD samples from mixtures stored for 1, 2, and 15 days, and recording of the spectra was done under static and flow-through conditions as well. The measurements have provided absorption cross sections in good agreement and so their average is proposed as the final result. This spectrum is presented in Figure 4.

As seen in Figure 4, 2,3PD has two broad absorption bands in the spectral range above ∼220 nm: one in the UV and the other one in the visible with maximum at 270 and 415 nm, respectively. There is some indication for a vibrational structure of the second band, which may have been blurred, however, by the relatively low resolution (∼0.4 nm) of our spectrometer. We have observed weak absorption extended to even longer wavelengths in the visible region but do not report the spectrum above 450 nm because of the large scatter and significant intercept of the BL-plots. The absorption spectrum of 2,3PD is similar to that of biacetyl in terms of the band positions, absorption cross sections and band widths.[33]

The only absorption spectrum that is available for 2,3PD from the literature has been reported by Jackson and Yarwood,[8] which is presented also in Figure 4. The UV-portion of the spectrum reported by these authors, a large peak at 253 nm with a shoulder at 280 nm, shows close resemblance to that we observed with the 2,3PD sample when used without purification. As discussed, the strong short-wavelength band was absent in the spectrum that we obtained with the purified 2,3PD. The absorption band lying at longer wavelengths shows significant disparity as well (Figure 4). We note that we have obtained the same spectrum with the purified sample and without purification above ∼350 nm. Clearly, this is not yet a proof for that our spectrum should be preferred at longer wavelengths as well.

**3.2.2. Pulsed Laser Photolysis Results.** The 351 nm PLP-QR experiments were performed at laboratory temperature ($T$ = 300 ± 2 K) in synthetic air at 1000 mbar total pressure to determine the photolysis quantum yield, $\Phi_2$(351 nm). The concentration of 2,3PD was measured before photolysis, [2,3PD]$_0$, and after $n$ laser shots, [2,3PD]$_n$, by GC analysis. Fresh gas mixtures were prepared for each irradiation. The experimental observables were evaluated according to eq VIII:[13,14]

$$\ln([2,3\mathrm{PD}]_n/[2,3\mathrm{PD}]_0) = -C \times \Phi_2(351\ \mathrm{nm}) \times (n \times E) \quad \text{(VIII)}$$

$$\text{with} \quad C = f_w(351\ \mathrm{nm}) \times E_{Ph}(351\ \mathrm{nm})^{-1} \times \sigma_{2,3PD}(351\ \mathrm{nm}) \times \ell \times V^{-1}$$

where $E$ is the laser energy (mJ) per pulse, $f_w$(351 nm) is the transmission of the entrance window (the measured value was 0.930 for one window), $E_{Ph}$(351 nm) is the energy of one photon (mJ photon$^{-1}$), $\ell$ (= 11.6 cm) is the optical path length, and $V$ is the total volume of the cell (cm$^3$). $\Phi_2$(351 nm) was obtained by plotting ln([2,3PD]$_n$/[2,3PD]$_0$) against ($n \times E$) and making use of the absorption cross section measured in the present work and the known parameters in eq VIII. A plot of ln([2,3PD]$_n$/[2,3PD]$_0$) versus ($n \times E$) is presented in Figure 5.

The reaction mixture contained 1-pentene in two experiments to trap the OH radicals potentially formed in the photo-oxidation system. Open symbols in Figure 5 represent the data obtained in the presence of OH-scavenger. The concentration of 1-pentene was 9.11 × 10$^{14}$ and 8.9 × 10$^{15}$ molecules cm$^{-3}$ at low and high


dx.doi.org/10.1021/jp205595c |J. Phys. Chem. A 2011, 115, 9160–9168

2,3PD depletion, respectively. The result is seen invariant to the absence or presence of the OH scavenger 1-pentene that is believed to be a strong indication for the reliability of the quantum yield determined in the PLP-QR experiments. Linear least-squares analysis of all data in Figure 5 has provided $\Phi_2(351\ \text{nm}) = 0.11 \pm 0.01$, where the error given represents $2\sigma$ statistical uncertainty. Systematic errors were assessed for the parameters used in eq VIII, for example, it is ±4% for the energy measurement judged by $NO_2$ actinometry. Root mean squares combination of the statistical and systematic errors gives ±20%, which is the proposed overall uncertainty at the $2\sigma$ (95% confidence) level. That is, the recommended quantum yield from our present study is:

$$\Phi_2(351\ \text{nm}) = 0.11 \pm 0.02$$

The "real" accuracy of the measurements can be considerable poorer than that given above due to the small absorption cross section of the 2,3PD molecule at the 351 nm photolysis wavelength.

**3.2.3. Broadband Photolysis Results.** Continuous photolysis of 2,3PD was carried out in the collapsible Teflon reactor in air buffer gas using fluorescent UV lamps with maximum emissions at 312 nm ($T = 300 \pm 2$ K, $P = 1000$ mbar, CP-TR experiments). The photolysis rate coefficient ("photolysis frequency"), $J_2$(312 nm), was determined by monitoring the loss of the photolyte via online GC analysis. Experiments were performed with and without adding 1-pentene to the irradiated gas mixtures. 1-Pentene served to trap the OH radicals that potentially formed in the reaction systems. The depletion of 2,3PD concentration has been found to follow first-order kinetics as shown in Figure 6,

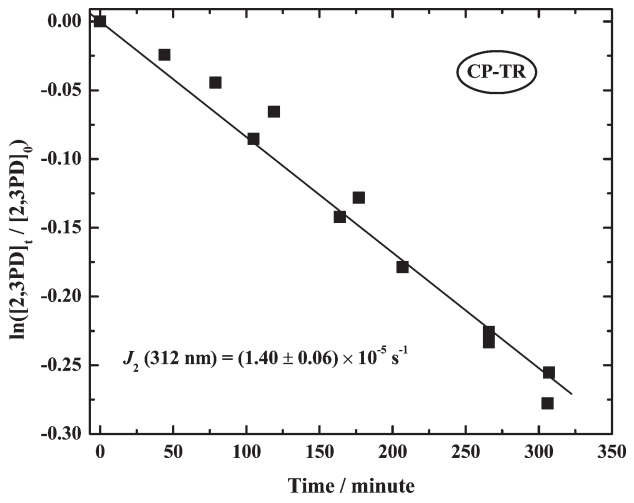


**Figure 6.** Depletion of 2,3PD concentration in the broadband photolysis experiments performed in the Teflon-film reactor at 312 nm. The reaction mixtures contained 1-pentene as an OH scavenger. The slope of the straight line gives the $J_2$ photolysis rate coefficient.

where the $\ln([2,3PD]_t/[2,3PD]_0)$ data are plotted against the reaction time, $t$, from two series of photolysis experiments. The $J_2$ values have been obtained by linear regression as the slope of the straight lines and are listed in the second column of Table 2.

The photolysis rate coefficient determined for 2,3PD is higher by ~30% in the absence of OH-scavenger. The OH radicals that caused the additional consumption of 2,3PD were probably formed via secondary reactions involving peroxy-radical chemistry in the photo-oxidation systems. The formation of OH by the primary photodissociation of 2,3PD can not be excluded either, but no products were determined in our current photolysis study to assess the primary and secondary photochemical processes. The photolysis rate coefficient determined in the presence of the OH scavenger is discussed next.

$J_2$ has been normalized to the photon flux by using $NO_2$ actinometry (note that the emission spectrum of the fluorescent lamps and the absorption spectra of 2,3PD and $NO_2$[19] overlap in a substantial wavelength range). A dilute mixture of $NO_2$ in atmospheric pressure $N_2$ buffer gas was photolyzed in the Teflon reactor under the very same irradiation conditions than those of the 2,3PD photolysis experiments and the concentration depletion of $NO_2$ was measured as a function of the photolysis time up to 15−20% conversion. A plot of $\ln[NO]_2$ versus $t$ yielded a straight line, the slope of which was equated to $J_{NO_2}$ after minor correction for secondary reactions as proposed by Holmes et al.[34,35] The determined $J_{NO_2}$ photolysis frequencies along with the ratios $J_2/J_{NO_2}$ are given in Table 2.

The $J_2/J_{NO_2}$ values in Table 2 have been utilized to estimate an "integral" or "effective" quantum yield,[36,37] $\Phi_2^{\text{eff}}$, for the photolysis of 2,3PD with the broad-band fluorescent lamp with $\lambda_{max} = 312$ nm and $w = 12$ nm maximal emission wavelength and a full width at half maxima, respectively. The following expression was used:

$$\Phi_2^{\text{eff}} = \frac{J_2}{J_{NO_2}} \times \left\{ \frac{0.5\sigma_{NO_2}(\lambda_{max} - 0.5w) + \sigma_{NO_2}\lambda_{max} + 0.5\sigma_{NO_2}(\lambda_{max} + 0.5w)}{0.5\sigma_{2,3PD}(\lambda_{max} - 0.5w) + \sigma_{2,3PD}\lambda_{max} + 0.5\sigma_{2,3PD}(\lambda_{max} + 0.5w)} \right\} \times \Phi_{NO_2} \quad \text{(IX)}$$

In eq IX, $\Phi_{NO_2}$ is the quantum yield for nitrogen dioxide photolysis, which was taken unity[19,37] over the whole wavelength range studied; the absorption cross sections of $NO_2$, $\sigma_{NO_2}(\lambda)$, were taken from ref 19 for the calculations and the $\sigma_{2,3PD}(\lambda)$ values from the present work (Table SI-1 in the Supporting Infrmation). The estimated effective quantum yield is $\Phi_2^{\text{eff}}(312\ \text{nm}) = 0.41 \pm 0.05$. Trial calculations have shown only small change of the effective quantum yields when more overlap between the emission spectrum of the lamp and the absorption spectra of $NO_2$ and 2,3PD were taken into account.

As discussed, there was a strong, albeit indirect, indication for the formation of OH radicals in the broadband photolysis study performed at 312 nm causing a potential overestimation of the

**Table 2. Photolysis Rate Coefficients and Effective Quantum Yields Determined in the Collapsible Teflon Reactor at 312 nm Using Broadband Fluorescent Lamps ($T = 300 \pm 2$ K, $P = 1000$ mbar Air)**

| OH scavenger | $J_2$[a] ($10^{-5}$ s$^{-1}$) | $J_{NO_2}$[a] ($10^{-3}$ s$^{-1}$) | $100 \times (J_2/J_{NO_2})$ | $\Phi_2^{\text{eff}}$[b] |
|---|---|---|---|---|
| no scavenger | 1.92 ± 0.08 (2) | 0.78 ± 0.01 (9) | 1.80 ± 0.12[d] | 0.41 ± 0.05[d] |
| 1-pentene[c] | 1.40 ± 0.06 (3) | | | |

[a] The number of experiments are given in the parentheses; 6 × 20 W lamps were used in the experiments. [b] Effective quantum yield (see text). [c] OH-scavenger: $[1\text{-pentene}]_0 = 9.1 \times 10^{14}$ molecules cm$^{-3}$. [d] Using $J_2$ values determined in the presence of OH scavenger.


dx.doi.org/10.1021/jp205595c | J. Phys. Chem. A 2011, 115, 9160–9168

quantum yields. In contrast, no such problem was observed in the PLP experiments at 351 nm. No obvious reason can be given to explain the diverse behavior. We just note that more photolysis channels are accessible at the lower wavelength studied (see next section) that may have led to different secondary photooxidation processes. The concentration of 1-pentene was not varied in the CP experiments, but it was assumed to be sufficiently high to scavenge all OH formed in the system. Thus, the determined quantum yield is proposed to be only an upper limit, that is, $\Phi_2^{eff}(312\ nm) \leq 0.41$.

**3.2.4. Photochemistry of 2,3PD.** We have determined photolysis quantum yields for 2,3-pentanedione using 351 nm XeF laser and 312 nm fluorescence lamps at room temperature ($T = 300 \pm 2$ K) in 1000 mbar air buffer gas with the results of $\Phi_2(351\ nm) = 0.11 \pm 0.02$ and $\Phi_2^{eff}(312\ nm) \leq 0.41$. These are high values for the studied wavelengths and pressure. They appear high in comparison, for example, with the long-wavelength photolysis quantum yields of monoketones[14] and the 365 nm quantum yield of the α-diketone biacetyl.[38] On the other side, however, high quantum yields have been reported for the photolysis of the α-ketoaldehyde, methylglyoxal, $CH_3C(O)C(O)H$, even at around 400 nm photolysis wavelength, although determined at lower pressures.[6] Clearly, further investigations are needed to determine accurate photolysis quantum yields for 2,3PD. Among the quantum yields determined, we give preference to that obtained by the laser photolysis method.

Consumption yields were measured and no photolysis products were determined in our current work. Thermochemistry and the scarce information available from the literature suggest channels 2a−2d to be primary photolysis channels for 2,3PD at the relatively low excitation energies of the investigations:

$$CH_3C(O)C(O)CH_2CH_3 + h\nu$$

$$\rightarrow CH_3CO + CH_3CH_2CO \quad \Delta_{2a}H^\circ_{298} = 302\ kJ\ mol^{-1}\ [19,39],\ \lambda_{threshold} = 395\ nm \qquad (2a)$$

$$\rightarrow CH_3CO + CH_3CH_2 + CO \quad \Delta_{2b}H^\circ_{298} = 344\ kJ\ mol^{-1}\ [19,39],\ \lambda_{threshold} = 346\ nm \qquad (2b)$$

$$\rightarrow CH_3C(O)C(O) + CH_3CH_2 \quad \Delta_{2c}H^\circ_{298} = 354\ kJ\ mol^{-1}\ [19,39,40],\ \lambda_{threshold} = 336\ nm \qquad (2c)$$


$$\Delta_{2d}H^\circ_{298} < 274\ kJ\ mol^{-1},\ \lambda_{threshold} > 435\ nm\ [41] \qquad (2d)$$

The applied photolysis wavelengths of 312 and 351 nm correspond to the excitation energies of 382 and 340 kJ $mol^{-1}$, respectively. Three different C−C photodissociation routes are energetically accessible at 312 nm excitation, channels 2a−2c, while at 351 nm, only the formation of $CH_3CO + CH_3CH_2CO$, channel 2a, is feasible at ambient temperatures. The free radical product $CH_3C(O)C(O)$ formed via channel 2c may undergo decomposition depending on its excess energy[3,40] to form $CH_3CO$ and CO. The photoisomerization reaction 2d may take place at both excitation wavelengths studied: this channel has been proposed by Turro and Lee in a classical liquid-phase photochemical study[41] (see below). (The reaction enthalpies for the different photolysis channels have been obtained by taking the recently published standard enthalpy of formation of $\Delta_f H^\circ_{298}(2,3PD) = -343.7 \pm 2.5$ kJ $mol^{-1}$ from ref 39 and the other enthalpy data from refs 19,39, and 40.)

Little is known about the photochemistry of 2,3PD from the literature. Turro and Lee[41] have studied the photochemistry of 2,3PD in solution at 435 nm. They have shown that photolysis of 2,3PD forms 1-hydroxy-1-methyl-2-cyclobutanone via an intramolecular photoreduction process, eq 2d, with a quantum yield of ∼0.06.[41] Jackson and Yarwood[42] have investigated the fluorescence and phosphorescence of 2,3PD in the gas phase at 365, 405, and 436 nm. They have derived a rate coefficient expression by the temperature dependent quenching of the phosphorescence of 2,3PD[42] consistent with the eq 2d photoisomerization process.[41] In an unpublished photo-oxidation study, performed at 254 nm in the Teflon reactor in our own laboratory, the build-up of acetaldehyde, $CH_3CHO$, was observed concomitant with the consumption of 2,3PD,[35] indicating the occurrence of photodissociation channels 2a−2c.

## 3.3. ATMOSPHERIC IMPLICATIONS

The absorption spectrum of 2,3-pentanedione extends to long wavelengths (Figure 4) where the solar flux increases rapidly in the troposphere, for example, the flux is ∼150 times higher at 400 nm than that at 300 nm at the Earth's surface. Also, as presented in sections 3.2.2−3.2.4, 2,3PD undergoes photochemical changes with quantum yields that are still fairly uncertain, but they are believed significant even at relatively long wavelengths. These factors imply a likely short photolysis lifetime of 2,3PD, $\tau_{phot}$, in the troposphere.

As discussed, we prefer the quantum yield determined with the monochromatic laser light, $\Phi_2(351\ nm) = 0.11 \pm 0.02$. We estimate $\tau_{phot}$[43] by assuming $\Phi_2$ to be 0.1 over the whole wavelength range of 290−450 nm and utilizing the measured absorption cross sections along with tabulated actinic fluxes taken from ref 43. This estimation has provided the photolysis lifetime of less than one hour for 2,3PD during daytime at mid latitudes on the ground level. The same qualitative result is obtained assuming 0.06 for the photolysis quantum yield[41] due to the significant absorption of 2,3PD and the high solar flux in the longer wavelength region.

Similar to other carbonyl molecules, OH-reaction can be an important initiation step for the tropospheric degradation of 2,3PD beside photolysis. The $k_1$ value determined at laboratory temperature can be used to estimate the tropospheric lifetime of 2,3PD with respect to its reaction with OH radicals, $\tau_{OH}$. With an average global OH concentration of $[OH]_{global} = 1 \times 10^6$ radicals $cm^{-3}$ (24 h average),[44] the tropospheric lifetime of $\tau_{OH} \approx 1/[k_1(300\ K) \times [OH]_{global}] = 5.3$ days is estimated.

In summary, our estimations show that photolysis is likely the dominant process to control the loss of 2,3PD in the troposphere. While this conclusion is believed correct in qualitative terms, accurate lifetime can not be given as yet, mostly because of the uncertainty of the photolysis quantum yields. It is noted also that the simple assessment used here is based on the assumption that 2,3PD is uniformly mixed through the troposphere that is probably not the case in view of the short lifetime of this OVOC and the average tropospheric transport time scale (1−2 months). The short lifetime indicates that 2,3PD will be removed rapidly close to its local sources in the atmosphere.

## ■ ASSOCIATED CONTENT

**Supporting Information.** Absorption cross sections for 2,3-pentanedione tabulated in 1 nm intervals along with representative Beer−Lambert plots; GC conditions; relative-rate plot to obtain $k_1(OH + 2,3PD)/k_3(OH + MEK)$. This material is available free of charge via the Internet at http://pubs.acs.org.

## AUTHOR INFORMATION

**Corresponding Author**
*E-mail: dobe@chemres.hu; alexandre.tomas@mines-douai.fr.

## ACKNOWLEDGMENT

This work has been supported in part by the Hungarian Research Fund OTKA (Contract OMFB-00992/2009). E.Sz. gratefully acknowledges the financial support from the French Foreign Office and Région Nord—Pas de Calais in the framework of the ARCUS program. The authors are indebted to the reviewers for their comments and helpful suggestions.

## REFERENCES

(1) Burdock, G. A. *Fenarolli's Handbook of Flavor Ingredients*, 5th ed.; CRC Press: Boca Raton, FL, 2005.
(2) Feierabend, K. J.; Zhu, L.; Talukdar, R. K.; Burkholder, J. B. *J. Phys. Chem. A* **2008**, *112*, 73.
(3) Baeza-Romero, M. T.; Glowacki, D. R.; Blitz, M. A.; Heard, D. E.; Pilling, M. J.; Rickard, A.; Seakins, P. W. *Phys. Chem. Chem. Phys.* **2007**, *9*, 4114.
(4) Dagaut, P.; Wallington, T. J.; Liu, R.; Kurylo, M. J. *J. Phys. Chem.* **1988**, *92*, 4375.
(5) Feierabend, K. J.; Flad, J. E.; Brown, S. S.; Burkholder, J. B. *J. Phys. Chem. A* **2009**, *113*, 7784.
(6) Chen, Y.; Wang, W.; Zhu, L. *J. Phys. Chem. A* **2000**, *104*, 11126.
(7) Klotz, B.; Graedler, F.; Sorensen, S.; Barnes, I.; Becker, K. H. *Int. J. Chem. Kinet.* **2001**, *33*, 9.
(8) Jackson, A. W.; Yarwood, A. J. *Can. J. Chem.* **1972**, *50*, 1331.
(9) Imrik, K.; Farkas, E.; Vasvári, G.; Szilágyi, I.; Sarzyński, D.; Dóbé, S.; Bérces, T.; Márta, F. *Phys. Chem. Chem. Phys.* **2004**, *6*, 3958.
(10) Dóbé, S.; Khachatryan, L.; Bérces, T. *Ber. Bunsen-Ges. Phys. Chem.* **1989**, *93*, 847.
(11) Pearlyn, D.; Pereira, D.; Kathirgamanthan, P. *J. Nat. Sci. Counc. Sri Lanka* **1977**, *5*, 41.
(12) Crunaire, S.; Tarmoul, J.; Fittschen, C.; Tomas, A.; Lemoine, B.; Coddeville, P. *Appl. Phys. B: Lasers Opt.* **2006**, *85*, 467.
(13) Gierczak, T.; Burkholder, J. B.; Talukdar, R. K.; Mellouki, A.; Barone, S. B.; Ravishankara, A. R. *J. Photochem. Photobiol., A* **1997**, *110*, 1.
(14) Nádasdi, R.; Zügner, G. L.; Farkas, M.; Dóbé, S.; Maeda, S.; Morokuma, K. *ChemPhysChem* **2010**, *11*, 3883.
(15) Ohbayashi, K.; Akimoto, H.; Tanaka, I. *J. Phys. Chem.* **1977**, *81*, 798.
(16) Baasandorj, M.; Griffith, S.; Dusanter, S.; Stevens, P. S. *J. Phys. Chem. A* **2009**, *113*, 10495.
(17) Szabó, E.; Zügner, G. L.; Szilágyi, I.; Dóbé, S.; Bérces, T.; Márta, F. *React. Kinet. Catal. Lett.* **2008**, *95*, 365.
(18) Atkinson, R.; Baulch, D. L.; Cox, R. A.; Crowley, J. N.; Hampson, R. F.; Hynes, R. G.; Jenkin, M. E.; Rossi, M. J.; Troe, J. *Atmos. Chem. Phys.* **2006**, *6*, 3625.IUPAC Subcommittee for Gas Kinetic Data Evaluation, http://www.iupac-kinetic.ch.cam.ac.uk.
(19) Sander, S. P.; Finlayson-Pitts, B. J.; Friedl, R. R.; Golden, D. M.; Huie, R. E.; Keller-Rudek, H.; Kolb, C. E.; Kurylo, M. J.; Molina, M. J.; Moortgat, G. K.; Orkin, V. L.; Ravishankara, A. R.; Wine, P. H. *Evaluation Number 15*, Jet Propulsion Laboratory: Pasadena, 2006.
(20) Darnall, K.; Atkinson, R.; Pitts, J. N. *J. Phys. Chem.* **1979**, *83*, 1943.
(21) Holloway, A.; Treacy, J.; Sidebottom, H.; Mellouki, A.; Daele, V.; Le Bras, G.; Barnes, I. *J. Photochem. Photobiol., A* **2005**, *176*, 183.
(22) Kung, J. F. T. *J. Agric. Food Chem.* **1974**, *22*, 494.
(23) Schwarzenback, G.; Wittwer, C. *Helv. Chim. Acta* **1947**, *30*, 656.
(24) Le Calvé, S.; Hitier, D.; Le Bras, G.; Mellouki, A. *J. Phys. Chem. A* **1998**, *102*, 4579.
(25) Wallington, T. J.; Kurylo, M. J. *J. Phys. Chem.* **1987**, *91*, 5050.
(26) Mellouki, A.; Le Bras, G.; Sidebottom, H. *Chem. Reviews* **2003**, *103*, 5077.
(27) Kwok, E.; Atkinson, R. *Atmos. Environ.* **1995**, *29*, 1685.
(28) Smith, I. W. M.; Ravishankara, A. R. *J. Phys. Chem. A* **2002**, *106*, 4798.
(29) Hansen, J.; Francisco, J. *ChemPhysChem* **2002**, *3*, 833.
(30) Galano, A.; Alvarez-Idaboy, J. R. *Applications of Theoretical Methods to Atmospheric Science. Adv. Quantum Chem.* **2008**, *55*, 245.
(31) Henon, E.; Canneaux, S.; Bohr, F.; Dóbé, S. *Phys. Chem. Chem. Phys.* **2003**, *5*, 333.
(32) Alvarez-Idaboy, J. R.; Cruz-Torres, A.; Galano, A.; Ruiz-Santoyo, Ma. E. *J. Phys. Chem. A* **2004**, *108*, 2740.
(33) Horowitz, A.; Meller, R.; Moortgat, G. K. *J. Photochem. Photobiol., A* **2001**, *146*, 19.
(34) Holmes, J. R.; O'Brien, R. J.; Crabtree, J. H.; Hecht, T. A.; Seinfeld, J. H. *Environ. Sci. Technol.* **1973**, *7*, 519.
(35) Szabó, E. Atmospheric kinetics and photochemistry of oxygenated volatile organic compounds. *Ph.D. Thesis*, University of Lille and University of Szeged, 2011 (submitted).
(36) Tadić, J.; Juranić, I.; Moortgat, G. K. *J. Photochem. Photobiol., A* **2001**, *143*, 169.
(37) Raber, W. H.; Moortgat, G. K. *Progress and Problems in Atmospheric Chemistry*; World Scientific Publishing Co.: Singapore, 1995.
(38) Sheats, G. F.; Noyes, W. A. *J. Am. Chem. Soc.* **1955**, *77*, 1421.
(39) Kercher, J.; Fogleman, E.; Koizumi, H.; Sztáray, B.; Baer, T. *J. Phys. Chem. A* **2005**, *109*, 939.
(40) Jagiella, S.; Zabel, F. *Phys. Chem. Chem. Phys.* **2008**, *10*, 1799.
(41) Turro, N. J.; Lee, T.-J. *J. Am. Chem. Soc.* **1969**, *91*, 5651.
(42) Jackson, A. W.; Yarwood, A. J. *Can. J. Chem.* **1971**, *49*, 987.
(43) Finlayson-Pitts, B. J.; Pitts, J. N., Jr *Chemistry of the Upper and Lower Atmosphere: Theory, Experiments, and Applications*; Academic Press: San Diego, 2000.
(44) Heard, D. E.; Pilling, M. J. *Chem. Rev.* **2003**, *103*, 5163.